RSC Advances

ROYAL SOCIETY OF CHEMISTRY

www.rsc.org/advances

RSC Advances

ARTICLE

Two-step Process for Programmable Removal of Oxygen Functionality of Graphene Oxide: Functional, Structural and Electrical Characteristics

Received 00th January 20xx,
Accepted 00th January 20xx

DOI: 10.1039/x0xx00000x

www.rsc.org/

Kashyap Dave[a], Kyung Hee Park[b], Marshal Dhayal[a†]

Here we report two step programmable reduction of graphene oxide (GO) which was synthesized by oxidation of graphite. X-ray photoelectron spectroscopic (XPS) analysis confirmed the synthesis of exfoliated graphene oxide (GO) by introduction of oxygen as carboxylic (-COOH), epoxy (C-O-C) and hydroxyl (-OH) groups. First step of GO reduction was achieved separately by (i) hydrazine (rGO_{11}) and (ii) sodium borohydride (rGO_{21}). Soda lime was used in the second stage reduction of (a) hydrazine reduced GO (rGO_{12}) and (b) sodium borohydride reduced GO (rGO_{22}) to remove the remaining carboxylic functionality from the rGO_{11} and rGO_{21} surface. XPS spectra of rGO_{21} showed decrease (38 to 30 %) in the oxygen whereas the further reduction of rGO_{21} with soda lime can further reduce the oxygen content. Quantitative analysis of C(=O)OX in GO shows about 43% proportion of carbon atoms in C1s as carboxylic functionality whereas the reduction of it with sodium borohydride reduced it to about 10%. The use of soda lime for both rGO_{11} and rGO_{21} had further reduced the carboxylic functionality. An increase in the proportion of carbon atoms as sp^2 and decrease in the oxygen functionality were controlled in two step process of reduction. A very good correlation in the conductivity of reduced GO with the % proportion of sp^2 carbon observed.

1. Introduction:

Since the discovery of the graphene, a two dimensional carbonic material has showed an increased interest because of its distinct properties and potential applications [1-3]. Several researchers had reported the potential use of graphene in ballistic transport at room temperature [4], high electron and hole mobility [5], as super capacitor [6], thin film transistors [7]. Functional groups at the surface of chemically synthesized graphene and tunable optical properties have advantages in biosensing and optoelectronics applications [8-10]. Several methods were used to synthesize graphene such as (i) zip remove from the carbon nanotube [11], (ii) micromechanical method to exfoliate graphite [12-13] and (iii) chemical vapor deposition [14-18]. The method used for production of graphene by zip removed from carbon nanotube can provide higher purity but still the challenges are many at the commercial production. The unzipping of single-wall carbon nanotubes can provide higher purity and again it is not a commercially viable method. The use of micromechanical method to exfoliate graphite can have graphite crystallite plane size in the order of 1mm and these are only used in research at the moment. Despite of several advantages of graphene, the large scale chemical synthesis of graphene with purity is still a challenging task.

The graphene synthesized by chemical vapor deposition methods has been used in several applications like photonics, nanoelectronics, transparent conductive layers, sensors, biomedical applications. Similarly chemically reduced graphene oxide has crystallite plane size of 100 µm are also used for coatings, paint/ink, making composites, transparent conductive layers, energy storage devices and biological applications. Extensive studies were carried out for graphene synthesis by chemical routes [19-24]. Studies showed that the reduction of GO via chemical methods removes most of the oxygen functionalities from the surface of graphene oxide [25-28].

Graphene production at the large scale may be possible by the chemical exfoliation of graphite. This includes, oxidation of graphite powder and followed by reduction by strong reducing reagents such as hydrazine [29,30], hydroquinone [31], sodium borohydride and its

[a] 1Clinical Research Facility, CSIR-Centre for Cellular and Molecular Biology, Hyderabad 500007, India.
[b] 2Department of Dental Materials and Medical Research Center for Biomineralization Disorders, School of Dentistry, Chonnam National University, Gwangju 61186, Korea.
† Corresponding Author (E-mail: marshal@ccmb.res.in, Tel: +91-(0)-271-92500 Fax: +91-(0)-40- 271-60591)

derivatives [32,33], lithium aluminium hydride [34], ascorbic acid [35,36], saccharides [37], norepinephrine [38], KOH [39], ethylenediamine [40], polyelectrolyte [41], protein [42], sodium citrate [43], plant extracts [44-46], metal/acid [47-54], melatonin [55], amino acids [56-59], bacterial respiration [60-65], thermal treatment [66], photocatalytic [67-71], sonochemical [72], laser [73-76], plasmas [77], lysozyme [78], electrochemical [79-81] electric current [82]. However, the complete removal of oxygen functionalities at the surface of graphene oxide has not achieved via reduction methods of GO. There were reports assessing the potential of two-step reduction for removal of selective functional groups, but still these process are poorly understood [83,84]. The graphene synthesized via chemical routes contains several impurities and it has a large number of disorders. Thus, the synthesis of large surface area sheets of graphene with high purity via chemical route is also very challenging.

The oxidation of graphite via chemical method introduces mainly carboxylic, aldehyde and ketonic functional groups at the edge and epoxide and hydroxyl groups at the basal plans of graphene oxide [85-90]. N_2H_4 and $NaBH_4$ were the most commonly used reducing agents for reduction of graphene oxide. The $NaBH_4$ has ability to reduce aldehyde, ketone and carboxylic groups into the hydroxyls groups whereas N_2H_4 can reduce epoxide groups and hydroxyls groups [91,92]. The above reported reducing reagents in the literature can remove most of the oxygen from the surface of GO but still a large proportion of carboxylic and hydroxyls groups may remain at the surface of graphene oxide.

Here we report two step programmable reduction of graphene oxide which was synthesized by oxidation of graphite. The main objective of the study was to target the removable of carboxylic acid from the surface of reduced graphene oxide. Uniqueness of this study was the use of soda lime for removing carboxylic functional group from the surface of reduced GO by decarboxylation [93]. First level of reduction of GO was obtained via chemical route by the separate use of (i) hydrazine and (ii) sodium borohydride. Physico-chemical nature of the synthesized graphene oxide and hydrazine and sodium borohydride reduced GO were characterized by different spectroscopic techniques. Subsequent effect of the soda lime on removal of carboxylic acid from the (i) hydrazine and (ii) sodium borohydride reduced GO was estimated by x-ray photoelectron spectroscopy. In this study, we further quantified the proportion of carbon as sp^2 and sp^3 in reduced GO and GO by XPS.

2. Materials and Methods:

2.1. Materials:

$NaBH_4$, hydrazine hydrate and soda lime were purchased from Sigma Aldrich. Graphite flakes were obtained from CDH. H_2SO_4 and hydrochloric acid (HCl) were obtained from RANKEM. $KMnO_4$ and H_2O_2 were purchased from MERCK and S D Fine-Chem Limited (SDFCL) respectively. Milli-Q water (18Mohm) was used as a solvent for all the experiments. All other chemicals were of analytical grade and purchased from local suppliers.

2.2 Synthesis of Exfoliated Graphite Oxide Sheets

Here, we have modified the hummer method for the synthesis of graphene oxide [20,94]. The H_2SO_4 (46 ml) was added in the mixture of graphite flakes (2g) and $NaNO_3$ (1 g), stirred at 0-4°C using an ice bath till the solution becomes homogeneous. Gradually 6 g of $KMnO_4$ was added to the homogeneous graphite solution in 7 h at ~20°C by carrying out reaction in an ice bath chamber during the reaction period. Further to this mixture, 6 g of $KMnO_4$ was added to the graphite homogeneous solution in 4 h at 35-40°C and stirred for another 8 h. This reaction mixture was allowed to cool to the room temperature (25 °C) and poured onto ice prepared from ~260 ml of Milli-Q water. Finally 6 ml of 30% H_2O_2 was added to complete the reaction. Then the mixture was filtered with whatman paper and filtrate was collected. The filtrate was washed with 10% HCl and ethanol. Finally the product was thoroughly washed with Milli-Q water. The wet graphite oxide was dried by vacuum at room temperature for 5 days.

2.3 Reduction of GO

2.3.1 Reduction of GO with $NaBH_4$ and Hydrazine Hydrate

Synthesized graphite oxide (200 mg) was added to 200 ml water and ultra sonicated for 3 h while maintaining the pH 8-9. $NaBH_4$ (1.600 g,62.2 mM) was added to well dispersed graphene oxide solution and stirred at 70-80 °C for 2 h. The reaction mixture was allowed to cool down to the room temperature and was filtered by whatman paper. Filtrate was washed with methanol and MQ water

and dried in vacuum at room temperature for 3 days. For reduction of GO by hydrazine, 200 mg of GO was dispersed in 200 ml water by sonicating for 3 hr and 2ml of 64.2 mM of hydrazine was added and the solution was continuously stirred at 95°C for 24 h. The reaction mixture was allowed to cool down to the room temperature and was filtered by whatman paper. Filtrate was washed with methanol and MQ water and dried in vacuum at room temperature for 3 days.

2.3.2 Reduction of hydrazine and $NaBH_4$ reduced GO by Soda Lime

The reaction of soda lime with rGO can be described as R-COOH + soda lime 2(NaOH/CaO) → RH + Na_2CO_3 + H_2O, where 'R' represents rGO with remaining COOH functionalities [93]. The decorboxilation of rGO by soda lime can add hydrogen 'RH' to the 'R' (conversion of CH_2 into CH_3) while removing carboxylic functionalities. 100 mg of $NaBH_4$ reduced graphene oxide were dissolved in 100 ml water by ultrasonication for 2 h. 60 mg of 6.2 mM soda lime at pH (7 to 8) was added and stirred at 45-50 °C for 1 h. To adjust the pH of the solution, 1 M NaOH and 1 M HCl was used. The solution was filtered by whatman filter papers and filtrate was subsequently washed with 1 M HCl, methanol and MQ waters. The material was dried by vacuum at room temperature for 3 days. 100 mg of hydrazine reduced graphene oxide were dissolved in 100 ml water by ultrasonication for 2 h. 30 mg of 3.1 mM soda lime at pH (7 to 8) was added and stirred at 45-50°C for 1 h. To adjust the pH of the solution, 1M NaOH and 1HCl was used in the same way discussed above. The solution was filtered by whatman filter papers and filtrate was subsequently washed with 1 M HCl, methanol and MQ waters. The material was dried by vacuum at room temperature for 3 days.

Using above methods for synthesis of graphene oxide and reduced graphene oxides, we have synthesized five different types of carbonic materials as: (i) Graphene oxide (**GO**), (ii) N_2H_4 reduced GO (**rGO_{11}**), (iii) $NaBH_4$ reduced GO (**rGO_{21}**), (iv) Soda lime reduced rGO_{11} (**rGO_{12}**) and (v) Soda lime reduced rGO_{21} (**rGO_{22}**). Above materials were dissolved in three different solvents (water, tetrahydrofuran (THF) and methanol) and optical images of these are shown in **Fig. 1**. After sonication of 10 min, hydrazine reduced graphene oxide showed relatively less solvability as compare to the $NaBH_4$ reduced GO. For both the soda lime reduced GO had showed very good solvability in all three solvents. The GO and reduced GO dissolved in water used for further characterized by Raman spectroscopy, UV-Visible Spectroscopy, ATR-FTIR Spectroscopy, TGA, XPS and XRD.

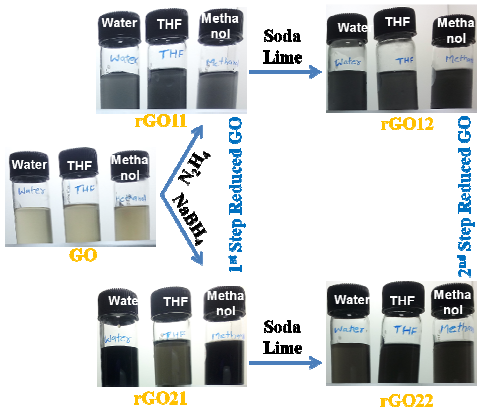

Fig 1. Optical images of graphene oxide (**GO**), N_2H_4 reduced GO (**rGO_{11}**), $NaBH_4$ reduced GO (**rGO_{21}**), soda lime reduced rGO_{11} (**rGO_{12}**) and soda lime reduced rGO_{21} (**rGO_{22}**) in three different solvents (water, THF and methanol).

2.4 Characterization

The order and disorder crystal structures of carbonic materials (graphite, graphene oxide and reduced graphene oxide) were characterized by Raman spectroscopy. Raman spectra of GO and reduced GO were measured by RENISHAW System at 532 nm laser. Absorption spectra of GO and reduced GO were measured by UV-2600 SHIMADZU Spectrophotometer. ATR-FTIR Spectroscope (Alpha-e Bruker System) was used to obtain the information about the surface functionalities of GO.

The crystallite structure of GO and reduced GO was characterized from XRD pattern. The XRD spectra were obtained by using a XRD-6000 (Japan) X-ray diffractometer in the diffraction angle range 5-80° with Cu-Kα radiation (λ= 1.54060 Å). Electrical characteristics of GO and reduced GO was characterized by taking same amount of the materials and solution casting in between the gold electrodes. The current was measured at different voltage and current voltage characteristic plotted. X-ray photoelectron spectra of GO and reduced GO were obtained by MultiLab200 with standard MgKα radiation to quantify elemental composition, surface carbon and oxygen functionalities. All spectra were taken at a working pressure of ~10^{-9} mbar. Wide scan XPS survey was used for elemental

proportion quantification and high-resolution spectra of C1s was used for characterization of surface functionalities. The different surface states were obtained in the high resolution C1s spectra by specifying a line shape, relative sensitivity factor, peak position, full width at half maxima, and area constraints.

3. Results and Discussion

Raman spectra of graphite, synthesized GO and reduced GO (rGO_{11}, rGO_{12}, rGO_{21} and rGO_{22}) were shown in **Fig. 2**. The Raman spectra of graphite show a sharp peak at 1576 cm^{-1} as in **Fig. 2**. Normally two distinct peaks in Raman spectra of graphite materials are observed due to (i) breathing of sp^2 atom of carbon (known as D band ~ 1360 cm^{-1}) and (ii) graphitic carbonic sp^2 of carbon atoms (known as G band ~ 1580 cm^{-1}) [94]. The peak at 1576 cm^{-1} corresponds to the G-band which represents stretching of the C-C bond. The conversion of graphite into graphene oxide induces several disorders in sp^2-hybridized carbon sheets; therefore an increase in D-band peak intensity of Raman spectra in GO occurs [29,95]. The Raman spectra of GO shows a wide peak at 1597 cm^{-1} due to stretching of the C-C bond present in aromatic ring of GO in all sp^2 carbon. The peak at 1358 cm^{-1} mainly associated with disorder introduced by addition of oxygen atom at the surface of graphite by oxidation process in GO. Observed ratio of the peak intensities of the D-band (I_D) with the G-band (I_G) peaks were 0.30 and 0.85 for graphite and GO, respectively. The relative peak intensity of D-band at 1358 cm^{-1} was increased as compared to G-band at 1597 cm^{-1} in GO in relation with graphite.

The Raman peak for D-band and G-band are at 1349 cm^{-1} and 1581 cm^{-1}, respectively for rGO_{11}. The measured intensity ratio of I_D/I_G for rGO_{11} was 1.17. The peak intensity of D-band as compared to the G-band in Raman spectra of rGO_{11} was relatively higher which is similar to previous finding [29]. A further reduction of rGO_{11} by soda lime which additionally deoxygenating the surface of rGO_{11} has showed a decrease (I_D/I_G ~1.08) in the intensity of D-band (at 1333 cm^{-1}) as compare to G band (at 1596 cm^{-1}) in Raman spectra of rGO_{12}. Raman spectra of $NaBH_4$ reduced GO (rGO_{21}) had a similar pattern to GO and D-band and G-band peaks are at 1355 cm^{-1} and 1589 cm^{-1}, respectively. The intensity ratio of I_D/I_G (~0.93) for rGO_{21} has slightly decreased as compared to rGO_{11}. The Raman peak position for D band and G bands are at 1331 cm^{-1} and 1599 cm^{-1}, respectively for rGO_{22} and the peaks intensity ratio I_D/I_G was ~1.14.

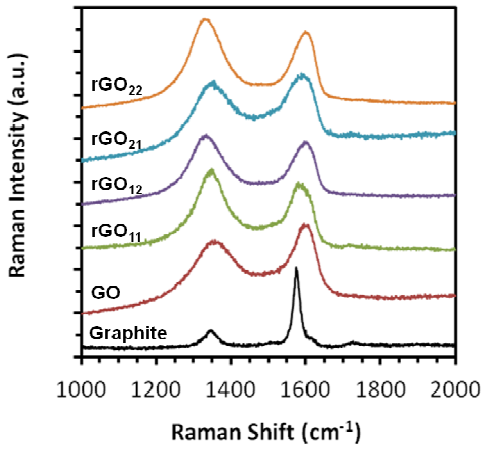

Fig 2. Raman spectra of graphite, graphene oxide (**GO**), N_2H_4 reduced GO (**rGO_{11}**), $NaBH_4$ reduced GO (**rGO_{21}**), soda lime reduced rGO_{11} (**rGO_{12}**) and soda lime reduced rGO_{21} (**rGO_{22}**).

The Raman spectra of GO showed a large red shift in the G-band position after oxidation of graphite into GO and results are shown in supporting information (**SFig.1**). Previously similar red shift was observed by Bo et al. [96]. Gupta et. al.[97] had explained the red shift of the G band in Raman spectra due to an increase in the number of layers of graphene. The change in Raman peak position and shape were used to estimate the number of layers of graphene [98]. Thus, the observed red shift in the G-band position of GO Raman spectra in our finding indicated an increase in the thickness of the layered structures of graphene oxide sheets. Reduction of GO by both the reducing agents (i) $NaBH_4$ and (ii) N_2H_4 had showed a decrease in the red shift of the D-band. The oxidation of graphite had showed red in D band whereas the further reduction of GO cause a blue shift in D band of the Raman spectra. This change may be due to change in sp^2 hybridize cluster size by addition / removal of oxygen functional groups from the surface in oxidation and reduction process. A further reductions with soda lime cause a large red shift in the spectra and D-band position are at 1596 and 1599 cm^{-1} for rGO_{12} and rGO_{22}. We do not understand the mechanism, but it could be due to multiple folding of highly reduced graphene oxide. Previous Raman peak at 1582-1600 cm^{-1} correspond to glass carbon in carbonic materials[99].

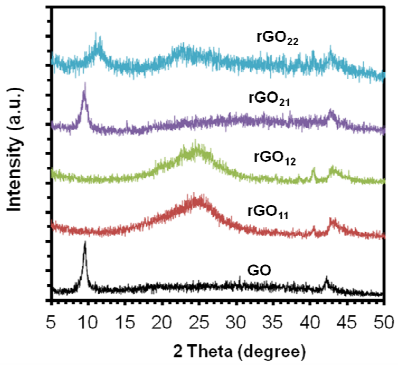

Fig 3. XRD spectra of graphene oxide (**GO**), N_2H_4 reduced GO (**rGO_{11}**), $NaBH_4$ reduced GO (**rGO_{21}**), soda lime reduced rGO_{11} (**rGO_{12}**) and soda lime reduced rGO_{21} (**rGO_{22}**).

XRD spectra of synthesized GO and reduced GO (rGO_{11}, rGO_{12}, rGO_{21} and rGO_{22}) are shown in **Fig. 3**. A sharp peak at $2\vartheta \sim 10^{o}$, corresponds to the reflection from the (002) plane, was observed in XRD spectra of GO[100]. Peak at $2\vartheta \sim 43^{o}$ may correspond to the turbostratic band of disordered carbon materials. XRD spectra of N_2H_4 reduced GO showed a wide peak at $2\vartheta \sim 43^{o}$ and the peak at $2\vartheta \sim 10^{o}$ was completely disappeared. Reduced graphene oxide has a peak around $2\vartheta \sim 23^{o}$. The broad diffraction peak of rGO indicates poor ordering of the sheets along the stacking direction. rGO_{21} XRD had a broad peak at $2\vartheta \sim 10^{o}$ with increased full width half maxima (FWHM). Further reduction of rGO_{21} with soda lime shows a peak shift towards higher 2ϑ and an increase in the peak broadening. This change in peak position and FWHM of the peak could be due to the exfoliation of GO sheets after removal of the intercalated carboxylic groups[101,102]. These XRD results are closely related to the exfoliation and reduction processes of GO.

Fig 4A shows UV-Vis spectra of synthesized GO and reduced GO (rGO_{11}, rGO_{12}, rGO_{21} and rGO_{22}) between the spectral range 200-700 nm. Absorbance peak of graphene oxide was present at 225 nm corresponds to the π-π^{*} transition and peak at 303 nm due to the transition in the C=O [103]. GO reduced by $NaBH_4$ and further by soda lime shows a peak shift at 262.5 nm and 263.5 nm, respectively. Reduction of GO by hydrazine and hydrazine with soda lime shows peak at 256 nm and 266.5 nm, respectively. Previous studies also showed a red shift in chemically reduced graphene oxide[64,68,71] and our experimental results are also consistence with previous observations.

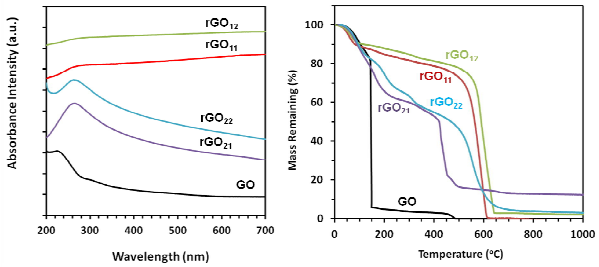

Fig 4. (A) UV-vis spectra and (B) TGA of graphene oxide (**GO**), N_2H_4 reduced GO (**rGO_{11}**), $NaBH_4$ reduced GO (**rGO_{21}**), soda lime reduced rGO_{11} (**rGO_{12}**) and soda lime reduced rGO_{21} (**rGO_{22}**).

Thermal stability of synthesized GO and reduced GO (rGO_{11}, rGO_{12}, rGO_{21} and rGO_{22}) was measured between the temperature 10 to 1000 °C by thermogravimetric analysis and results are shown in **Fig 4B**.The thermal stability data of GO had shows maximum weight % loss due to higher number of oxygen and pyrolysis of liable oxygen functional groups at 150 °C. Further increase in the temperature shows a very small decrease in the remaining mass which may be due to release of CO and CO_2 gases. The comparative data for rGO_{11} and rGO_{12} had shows about 50 % of weight loss at 430 and 520 ^{o}C, respectively. These results suggest that the less number of oxygen groups present in rGO_{12} as compared to rGO_{11}. Similar observations were recorded for rGO_{21} and rGO_{22}.

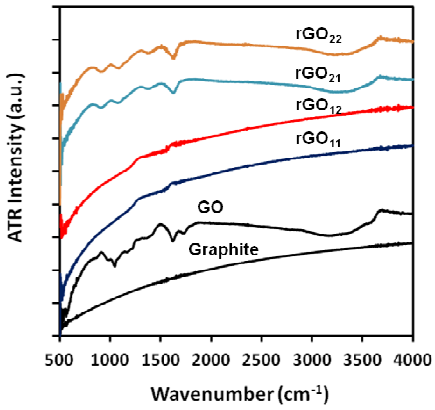

Fig 5. ATR-FTIR spectra of graphite, graphene oxide (**GO**), N_2H_4 reduced GO (**rGO_{11}**), $NaBH_4$ reduced GO (**rGO_{21}**), soda lime reduced rGO_{11} (**rGO_{12}**) and soda lime reduced rGO_{21} (**rGO_{22}**).

Fig.5 shows ATR-FTIR spectra of graphite, synthesized GO and reduced GO (rGO_{11}, rGO_{12}, rGO_{21} and rGO_{22}). The absence of any functional group in the ATR-FTIR spectrum of graphite was

observed. Oxidation of graphite show peaks at 1035, 1390, 1635 and 1751 cm^{-1} in the ATR-FTIR spectrum. The peak at 1751 cm^{-1} corresponds to the saturated carboxylic acids and peak at 1635 cm^{-1} correspond to $H_2C=CH_2$. Peaks at 1035 and 1390 cm^{-1} may be due to the presence of C-O and C=O. The presence of different oxygen functional groups and an increase in D-band of Raman spectra confirms the conversion of graphite into graphene oxide by the oxidation process used in this study. The ATR-FTIR spectra of rGO_{12} obtained after reduction of GO with N_2H_4 showed a very wide peak between 1300-1700 cm^{-1}. The disappearance of several functional peaks and the week peak intensity between 1300-1700 cm^{-1} confirms the removal of oxygen from the surface of GO by reduction process. A small peak at 1255 cm^{-1} is due to the presence of C-O. The FTIR result suggests that the maximum numbers of oxygen functionalities were removed from the surface of GO after reduction. The use of soda lime for further removal of carboxylic functional groups from the surface of reduced GO (rGO_{12}).

The strong appearance of the peak at 1645 cm^{-1} in $NaBH_4$ reduced GO (rGO_{21}) ATR-FTIR spectrum indicates that the reduced GO has mainly $H_2C=CH_2$. A peak at 905 in the spectra was assigned to the alkenes in the reduced GO sample. Two small peaks at 1373 and 1108 cm^{-1} could be associated with the C-O and -OH which indicating the presence of small proportion of oxygen groups at $NaBH_4$ reduced GO surface. ATR-FTIR spectra of soda lime deoxygenated $NaBH_4$ reduced GO (rGO_{22}) samples was very similar to the $NaBH_4$ reduced GO ATR-FTIR spectra as shown in **Fig 5**. Peak intensity at 1373 cm^{-1} was slightly reduced whereas a small increase in the peak intensity at 1645 cm^{-1} was observed. XPS analysis was carried out for quantitative analysis of carbon functionalities of GO and rGO.

Wide scan XPS spectra of synthesized GO and reduced GO (rGO_{11}, rGO_{12}, rGO_{21} and rGO_{22}) were obtained to further quantify the chemical nature of GO and reduced GO. Wide scan XPS spectra of these are shown in supporting information (**SFig. 2**). Oxygen to carbon elemental percentage proportions in synthesized GO was 38% and 62%, respectively. XPS wide scan spectra of GO reduced with $NaBH_4$ shows significant decrease (38 to 30 %) in the oxygen content at the surface. About 11% (atomic percentage) of oxygen was observed in N_2H_4 treated GO whereas before reduction it was 38% (atomic percentage). A further reduction of rGO_{21} with soda lime can further reduce the oxygen content at the surface of rGO. In contrary to the $NaBH_4$, the use of N_2H_4 can reduce the higher proportion of oxygen content from the surface of GO.

High resolution XPS spectra of C1s of synthesized GO and reduced GO were obtained. The peak fitting for surface state quantification from C1s was done as described in previous studies[104] and results are shown in **Fig 6**. C1s peak mainly fitted as hydrocarbon (CC), hydroxyl (COX), C=O/O-C-O and carboxylic functionality peaks [105-107]. In our analysis and peak fitting, we have separately fitted two peaks of hydrocarbons as C1s (sp^2) and C1s (sp^3) for a better representation of the XPS observations [108]. An additional peak at the tail of the spectra towards higher binding energy which know as shake-up peak associated with carbon in aromatic ring was also separately assigned during the peak fitting [109]. Thus, the higher resolution C1s XPS spectra of GO was fitted with six peaks of different carbon environments as: hydrocarbon (C=C) at 283.5 eV, (C-C/C-H) at 285.7 eV, (C-OX) at 287.4 eV, (C=O/O-C-O) at 288.9 eV, (C(=O)OX) at 290.8 eV and satellite peak at 293.5 eV due to pi-pi interactions. The positions of each peak associated with C-OX, (C=O/O-C-O) and (C(=O)OX) were fixed by assigning 1.5±0.3 eV shift in the binding energy, respectively [110]. Previously Chu et. al. [108] had characterized amorphous and nanocrystalline carbon films and observed about ~1.7 eV difference in the binding energy associated with C1s (sp^2) and C1s (Sp^3) peak of carbon. During peak fitting we have observed about ~1.7±0.3 eV difference in the binding energy for C1s (sp^2) and C1s (sp^3). The percent proportion of different carbon environments in C1s was 8.3, 17.7, 13.2, 17.6 and 42.1 corresponds to the C=C, C-C/C-H, C-OX, C=O/O-C-O and C(=O)OX, respectively.

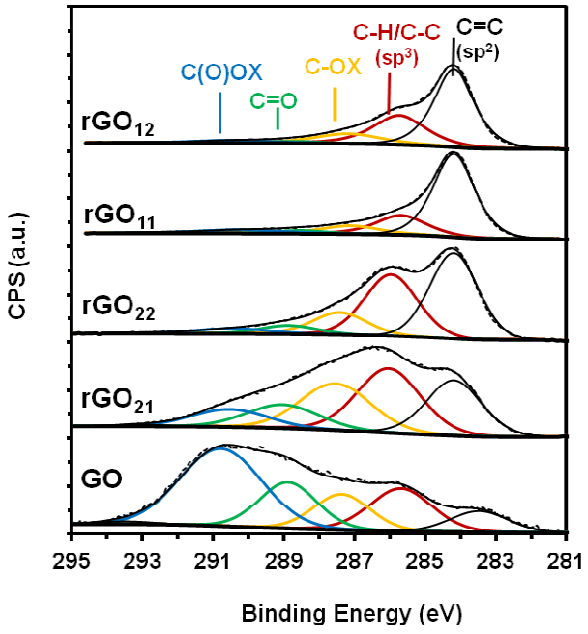

Fig 6. Peak fitted C1s XPS spectra of graphene oxide (**GO**), N_2H_4 reduced GO (**rGO$_{11}$**), $NaBH_4$ reduced GO (**rGO$_{21}$**), soda lime reduced rGO_{11} (**rGO$_{12}$**) and soda lime reduced rGO_{21} (**rGO$_{22}$**).

The higher resolution C1s XPS spectra of $NaBH_4$ reduced GO was fitted with six peaks of different carbon environments and the values for hydrocarbon (C=C) at 284.2 eV, (C-C/C-H) at 286.1 eV, (C-OX) at 287.6 eV, (C=O/O-C-O) at 289.1 eV, (C(=O)OX) at 290.6 eV and shake-up peak was at 293.2 eV. The percent proportion of different carbon environments in C1s was 22.9, 30.1, 24.2, 12.4 and 9.7 corresponds to the C=C, C-C/C-H, C-OX, C=O/O-C-O and C(=O)OX, respectively. The higher resolution C1s XPS spectra of soda lime reduced rGO_{21} was also fitted with similar six peaks as: hydrocarbon (C=C) at 284.2 eV, (C-C/C-H) at 286 eV, (C-OX) at 287.4 eV, (C=O/O-C-O) at 288.9 eV, (C(=O)OX) at 290.5 eV and a shake-up peak at 293.1 eV due to aromatic carbon atoms. The percent proportion of different carbon environments in C1s was 43.9, 34.1, 12.6, 4.9 and 3.8 corresponds to the C=C, C-C/C-H, C-OX, C=O/O-C-O and C(=O)OX, respectively.

The higher resolution C1s XPS spectra of N_2H_4 reduced GO was fitted as: hydrocarbon (C=C) at 284.2 eV, (C-C/C-H) at 285.7 eV, (C-OX) at 287.1 eV, (C=O/O-C-O) at 288.6 eV, (C(=O)OX) at 290.3 eV and shake-up peak at 292.8 eV. The percent proportion of different carbon environments in C1s was 64.8, 17.2, 8.4, 3.2 and 5.6 corresponds to the C=C, C-C/C-H, C-OX, C=O/O-C-O and C(=O)OX, respectively. The C1s XPS spectra of soda lime reduced rGO_{11} was fitted as: hydrocarbon (C=C) at 284.2 eV, (C-C/C-H) at 285.8 eV, (C-OX) at 287.2 eV, (C=O/O-C-O) at 288.3 eV, (C(=O)OX) at 290.5 eV and shake-up peak at 292.9 eV. The percent proportion of different carbon environments in C1s was 56.4, 26.9, 11.1, 1.9 and 3.7 corresponds to the C=C, C-C/C-H, C-OX, C=O/O-C-O and C(=O)OX, respectively. The XPS spectra of GO showed a spectra shift towards lower binding energy which may be due to insulating nature of sample [111.] However, there was no spectral shift was observed in reduced GO which indicates conducting nature of reduced GO.

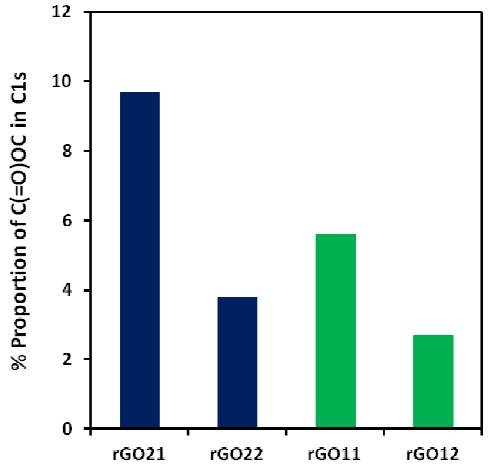

Fig 7. Percent proportion of carboxylic functionalists in C1s XPS spectra of N_2H_4 reduced GO (**rGO$_{11}$**), $NaBH_4$ reduced GO (**rGO$_{21}$**), soda lime reduced rGO_{11} (**rGO$_{12}$**) and soda lime reduced rGO_{21} (**rGO$_{22}$**).

Fig.7 shows quantitative analysis of C(=O)OX in synthesized GO and reduced GO (rGO_{11}, rGO_{12}, rGO_{21} and rGO_{22}). The synthesized GO has about 43 % proportion of carbon atoms in C1s as carboxylic functionality whereas the reduction of it with $NaBH_4$ reduced it to about 10 %. The use of soda lime further reduced the % proportion of carboxylic functionality. The rGO_{11} had showed a very low percentage of carboxylic functionality as compare to $NaBH_4$ reduced GO. The reaming carboxylic functionalities of rGO_{11} and rGO_{21} further reduced by soda lime and low level of carboxylic functionalities were achieved. Soda lime had reduced the carboxylic group significantly in both $NaBH_4$ and N_2H_4 reduced GO. An increase in the proportion of carbon atoms as sp^2 and decrease in the oxygen functionality was controlled in two step process in much more precise way. Table 1 shows comparison of D and G band shifts

in Raman spectra, peak intensity ratio of D to G Raman band and oxygen functionalities for different rGO.

Table 1. D and G Raman band shifts and oxygen functionalities for different rGO.

Code	Raman D-Band (cm^{-1})	Raman G-Band (cm^{-1})	I_D/I_G[a]	XPS COOX[b] (%)
rGO_{11}	1349	1581	1.17	5.6
rGO_{12}	1333	1596	1.09	2.7
rGO_{21}	1355	1589	0.94	9.7
rGO_{22}	1331	1599	1.14	3.8

[a] Experimentally observed peak intention ratio of D- band (I_D) and G- band (I_G) from Raman spectra and [b] percentage proportion of carboxylic functionalities in C1s XPS spectra.

Fig.8 showing I-V characteristics of GO and reduced GO (rGO_{11}, rGO_{12}, rGO_{21} and rGO_{22}). As expected, the GO did not show current conduction whereas the IV response of hydrazine reduced GO (rGO_{11}) showed a liner response. Two step increase in the current response of rGO_{12} observed. IV response of rGO_{21} was very distinct from the rGO_{11} and rGO_{12}. Initially a low current conduction was observed upto the 2V volt bias. A further increase in the bias voltage showed a rapid increase in the current and reached on saturation at 4V bias voltage.

Change in the relative conductivity of different types of reduced GO assessed by comparison of current at contact bias voltage in IV response curve. The conductivity of different types of reduced GO was observed according to the chemical and structural nature of the reduced GO. A very good correlation in the conductivity of reduced GO with the % proportion of SP^2 carbon obtained from XPS analysis was observed (supporting information **SFig. 3**). The two step process of reduction described here may provides an improvement and better structural, functional and electrical properties control in the reduction of GO. The two step process of reduction described here may provide a better conversion of graphite into graphene.

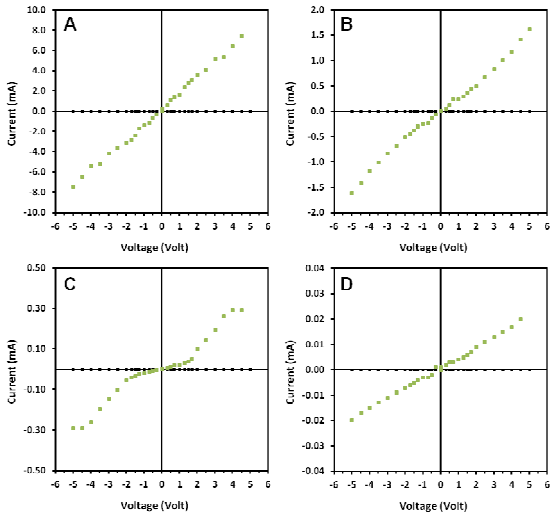

Fig.8 IV response of GO (black squire) and reduced GO (green squire). (A) rGO_{11}, (B) rGO_{12}, (C) rGO_{21} and (D) rGO_{22}.

Conclusions

Here we have described a method for a synthesis of chemically reduced graphene oxide which has higher proportion of graphene. First we have prepared highly exfoliated graphene oxide from graphite which was reduced by hydrazine and sodium borohydride. The Raman spectroscopic and XPS analysis confirm the synthesis of exfoliated graphene oxide by chemically introduced oxygen as carboxylic groups (-COOH), hydroxyl (–OH) and epoxy groups (C-O-C). Two distinct peaks of graphene oxide and reduced graphene in Raman spectra present due to breathing mode of sp^2 atom and graphitic carbonic sp^2 of carbon atoms. Raman spectra of hydrazine reduced GO showed relatively higher intensity of D-band as compare to the G-band in the spectra. A strong red shift in the G-band position was observed after oxidation of graphite into GO due to increase in the number of layers of graphene. The reduced GO by both reducing agent $NaBH_4$ and N_2H_4 had showed a decrease in the red shift of the D-band due to decrease in the thickness of the reduced GO sheets. The synthesized GO has very high % proportion of carbon atoms as carboxylic functionality whereas the reduction of it with $NaBH_4$ and Hydrazine is less. Soda lime had reduced the carboxylic group significantly in both $NaBH_4$ and N_2H_4 reduced GO. The two step process of reduction described here provides an improvement in the reduction of GO, therefore better conversion of graphite into graphene.

Acknowledgements

This work was supported by network project (NanoSHE) of Council for Scientific and Industrial Research (CSIR), Ministry of Science and Technology, Govt. of India. #KD is a Project Student at CCMB from Centre for Converging Technologies, University of Rajasthan, Jaipur 302004, India. The acknowledgements come at the end of an article after the conclusions and before the notes and references.

Notes and references

1 A.K. Geim. *Science,* 2009, **324**, 1530.
2 Y. Zhu, S. Murali, W. Cai, X. Li, J.W. Suk, J.R. Potts, Rodney S. Ruoff. *Adv. Mater.*, 2010, **22**, 3906.
3 H. Raza. Springer: NanoScience and Technology, 2012.
4 J.Baringhaus, M. Ruan, F.Edler, Tejeda, Sicot M, A.Taleb-Ibrahimi, A.P.Li, Z.Jiang, E.H.Conrad, C.Berger, C. Tegenkamp, W.A. Heer.. *Nature* , 2014,**506(7488),**349-54.
5 Y.Zhang, Y.W.Tan, H.Stormer and P.Kim. *Nature*, 2005,**438**, 201-204
6 B.T.Yu and J.M.Lee. *J. Mater. Chem. A*, 2013,**1**,14814-14843.
7 G.Eda, G.Fanchini and M.Chhowalla.*Nature Nanotechnology*, 2008,**3**,270-4.
8 Y.Liu, D.Yu, C.Zeng, Z.Miao and L.Dai. Langmuir 2010,**26(9)**,6158-6160.
9 S.W.Crowder, D.Prasai, R.Rath, D.A. Balikov, H.Bae, K.Bolotin and H.Sung .*Nanoscale*, 2013,**5(10)**,4171-6.
10 M.Zhang, B.Yin, X. Wang and B. Ye *Chem. Commun.* 2011,**47**,2399-2401.
11 D.V.Kosynkin, A.L. Higginbotham, A. Sinitskii, J.R. Lomeda, A. Dimiev, B.K.Price and J. M. Tour. *Nature* ,2009,**458**,872-876.
12 K.S.Novoselov, A.K.Geim, S.V.Morozov, D.Jiang, M.I.Katsnelson, I.V.Grigorieva, S.V. Dubonos and A.A.Firsov Nature 2005,438,197–200.
13 Y.Zhang, J.P.Small, M.E.S.Amori and P.Kim. *Phys. Rev. Lett*. 2005,**94,**176803.
14 A.Reina, X.Jia, J.Ho, D.Nezich, H.Son, V.Bulovic, M.S.Dresselhaus and J.Kong. *Nano Lett.* 2009,**9**,30–35.
15 J.C.Delgado, J.M.R.Herrera, X.Jia, D.A Cullen., H.Muramatsu, Y.A.Kim, T.Hayashi, Z.Ren, D.J.Smith, Y.Okuno, T.Ohba, H. Kanoh, K.Kaneko, M.Endo, H.Terrones, M.S.Dresselhaus and M.Terrones. *Nano Lett.* 2008,**8**,2773–2778.
16 N.G.Shang, P.Papakonstantinou, M.McMullan, M.Chu, A.Stamboulis, A. Potenza, S.S.Dhesi and H.Marchetto *Adv. Funct. Mater*. 2008,**18**, 3506–3514.
17 K.S.Kim, Y.Zhao, H.Jang, S.Y.Lee, J.M.Kim, K.S.Kim, J.H.Ahn, P.Kim, J.Y.Choi and B.H.Hong. *Nature* 2009,**457,**706–710.
18 W.Cai, R.D Piner., F.J.Stadermann, S.Park, M.A.Shaibat, Y.Ishii, D.Yang ,A.Velamakanni, S. J.An, M.Stoller, J.An, D.Chen, and R. S.Ruoff. *Science* 2008, **321**, 1815–1817.
19 B.C. Brodie. *Ann Chim Phys* 1860,**59**,466–72.
20 W.Hummers and R.Offeman. *J Am Chem Soc* 1958,**80**,1339.
21 L.Staudenmaier *Ber Dtsch Chem Ges* 1898,**31**,1481–99.
22 A.B.Bourlinos, D.Gournis, D. Petridis, T.Szabo, A.Szeri and I.Dekany. *Langmuir* 2003,**19(15),**6050–5.
23 U.Hofmann and A.Frenzel. *Kolloid-Z* 1934,**68**,149–51.
24 P.Xiao, M.Xiao, P.Liu and K.Gong. *Carbon* 2000,**38(4),**626–8.
25 N.A.Kotov, I.Dekany and J.H.Fendler.*Adv Mater* 1996,**8(8**),637–41.
26 A.Celzard. *Carbon* 2002**,40,**2801–15.
27 D.S.McLachlan. *J Phys C: Solid State Phys* 1986,**19(9**),1339–54.
28 McLachlan D.S.. *J Phys C: Solid State Phys* 1987,**20(7),**865–77.
29 S.Stankovich, D.A.Dikin, R.D.Piner, K.A.Kohlhaas, A.Kleinhammes, Y.Jia, Y.Wu, S.T.Nguyen and R.S.Ruoff. *Carbon* 2007,**45,**1558−1565.
30 S.Gilje, S.Han, M.Wang, K.L.Wang and R.B.Kaner. *Nano Lett*. 2007,**7,**3394−3398.
31 G.Wang, J.Yang, J.Park, X.Gou, B.Wang, H.Liu and Y. J.Facile. *J. Phys. Chem. C* 2008,**112**,8192−8195.
32 J.H.Shin, K.K.Kim, A.Benayad, S.M.Yoon, H.K.Park, I.S.Jung, M.H.Jin, H.K.Jeong, J.M.Kim, J.Y.Choi and Y.H.Lee. *Adv Funct Mater* 2009,**19,**1987–1992.
33 C.K.Chua and M.Pumera. *Mater Chem A* 2013,1,1892.
34 A.Ambrosi, C.K.Chua, A.Bonanni and M.Pumera. *Chem. Mater*. 2012**,24,**2292−2298.
35 M.J.F.Merino, L.Guardia, J.I.Paredes, S.V.Rodil, P.S.Fernández, A.M.Alonso and J.M.D.Tascón. *J Phys Chem C* 2010,**114**,6426−6432.
36 J.Gao, F.Liu, Y.Liu, N.Ma, Z.Wang and X.Zhang. *Chem Mater* 2010,**22**,2213−8.
37 C.Zhu, S.Guo, Y.Fang and S.Dong. *ACS Nano* 2010,**4**,2429−37.
38 S.M.Kang, S.Park, D.Kim, S.Y.Park, R.S.Ruoff and H.Lee. *Adv Funct Mater* 2011,**21**,108−112.
39 X.Fan, W.Peng, Y.Li, X.Li, S.Wang, G.Zhang and F.Zhang. *Adv Mater* 2008,**20**,4490−4493.
40 J.F.Che, L.Y.Shen and Y.H.Xiao. J Mater Chem 2010,**20**,1722–1727.
41 S.Zhang, Y.Shao, H.Liao, M.H.Engelhard, G.Yin and Y.Lin. *ACS Nano* 2011,**5**,1785–1791.
42 J.Liu, S.Fu, B.Yuan, Y.Li and Z.Deng. *J. Am. Chem. Soc*., 2010,**132**,7279–7281.
43 W.Wan, Z.Zhao, H. Han, Y.Gogotsi and J.Qiu. *Materials Research Bulletin* 2013,**48**,4797–4803.
44 Y.Wang, Z.Shi and J.Yin, *ACS Appl Mater Interfaces*, 2011**,3,**1127-1133.
45 S.Thakur and N.Karak. *Carbon,* 2012,**50**,5331-5339.
46 B.Haghighi and M.A.Tabrizi. *RSC Adv* 2013,**3**,13365-13371.
47 Z.Fan, K.Wang, T.Wei, J.Yan, L.Song and B.Shao. *Carbon* 2010,**48**, 1686-9.
48 Z.J.Fan, W.Kai, J.Yan, T.Wei, L.J.Zhi, J.Feng, Y.M.Ren, L.P.Song and F.Wei. *ACS Nano* 2010,**5**,191-8.
49 X.Mei and J.Ouyang. *Carbon* 2011,**49**,5389-5397.
50 P.B.Liu, Y.Huang and L.Wang .*Mater Lett* 2013,**91**,125-8.
51 R.S Dey.,S.Hajra, R.K.Sahu, C.R.Raj and M.K.Panigrahi *Chem Commun* 2012, **53**,1787-9.
52 N.A.Kumar, S.Gambarelli, F.Duclairoir, G.Bidan and L.Dubois. *J. Mater. Chem. A*, 2013,**1**,2789-2794.
53 V.H.Pham, H.D.Pham, T.T.Dang, S.H.Hur, E.J.Kim, B.S.Kong, S.Kim and J.S.Chung. *J Mater Chem* 2012,**22,**10530-6.
54 B.K.Barman, P.Mahanandia and K.K. Nanda *RSC Adv* 2013,**3**,12621-4.
55 A.Esfandiar, O.Akhavan and A.Irajizad. *J Mater Chem* 2011,**21**,10907-10914.
56 D.Chen, L.Li and L.Guo *Nanotechnology* 2011,**22**,325601.
57 S.Bose, T.Kuila, A.K.Mishra, N.H.Kim and J.H.Lee. *J Mater Chem* 2012,**22**,9696-9703.
58 J.K.Ma, X.R.Wang, Y.Liu, T.Wu, Y.Liu, Y.Q.Guo, R.Q.Li, X.Y.Sun , F.Wu, C.B.Li and J.P.Gao. *J Mater Chem A* 2013,**1,**2192–2201.
59 T.A.Pham, J.S.Kim, J.S.Kim ,Y.T.Jeong *Colloids Surf A: Physicochem Eng Aspects* 2011,**384**,543–8.
60 E.C.Salas, Z.Sun, A.Luttge and J.M.Tour. *ACS Nano* 2010,**4**,4852–6.
61 G.Wang, F.Qian, C.Saltikov, Y.Jiao and Y.Li. *Nano Res* 2011, **4,** 563–570.
62 O.Akhavan and E.Ghaderi. *Carbon* 2012,**50**,1853–1860.
63 S.Gurunathan, J.W.Han, V.Eppakayala and J.H.Kim. *Colloids Surf B* 2013,**102**,772–7.
64 P.Khanra, T.Kuila, N.H.Kim, S.H.Bae, D.S.Yu, J.H.Lee,. *Chem. Eng. J.,* 2012,**183**, 526–33.
65 Kuila T. Bose S. Khanra P. Mishra A.K., Kim N.H. and Lee J.H. *Carbon* 2012,**50**,914–21.
66 H.C.Schniepp, J.L.Li, M.J.McAllister, H.Sai, M.H.Alonso and D.H.Adamson. *J Phys Chem B* 2006,**110(17)**,8535–9.

67 G.Williams, B.Seger and P.V.Kamat. *ACS Nano* 2008,**2**,1487–91.
68 X.Huang, X.Zhou, S.Wu, Y.Wei, X.Qi, J.Zhang, F.Boey and H.Zhang *Small* 2010,**6**,513–516.
69 O.Akhavan and E.Ghaderi. *J Phys Chem C* 2009,**113**,20214–20220.
70 S.R.Kim, M.K.Parvez and M.Chhowalla. *Chem Phys Lett* 2009,**483**,124–127.
71 H.B.Yao, L.H.Wu, C.H.Cui, H.Y.Fang and S.H.Yu. *J Mater Chem,* 2010,**20**,5190–5195.
72 K.Vinodgopal, B.Neppolian, I.V.Lightcap, F.Grieser, M.A.kumar and P.V.Kamat. *J Phys Chem Lett* ,2010,**1**,1987–1993.
73 D.A.Sokolov, K.R.Shepperd and T.M.Orlando. *J Phys Chem Lett* 2010,**1**,2633–6.
74 Y.Zhou, Q.Bao, Varghese, Tang LAL, C.K.Tan, C.H.Sow and K.P.Loh. *Adv Mater*, 2010,**22**,67–71.
75 Y.Zhang, L.Guo, S.Wei, Y. He, H.Xia, Q.Chen, H.B.Sun and F.S Xiao.. *Nano Today* 2010,5, 15–20.
76 V.Abdelsayed, S.Moussa, H.M.Hassan, H.S.Aluri, M.M.Collinson, M.S.E.Shall. *Chem Lett* 2010,1,2804–2809.
77 M.Baraket, S.G.Walton, Z.Wei, E.H.Lock, J.T.Robinson and P.Sheehan .*Carbon* ,2010,**48**,3382–3390.
78 F.Yang, Y.Liu, L.Gao and J. Sun. *J Phys Chem C* ,2010,**114**,22085–91.
79 C.Fu, Y.Kuang, Z.Huang, X.Wang, N.Du, J.Chen and S.Zhou . *Chem Phys Lett* 2010,499,250–3.
80 M.Zhou, Y.Wang, Y.Zhai, J.Zhai, W.Ren, F.Wang and S. Dong. *Chemistry - A European Journal* ,2009,15,6116–20.
81 L.Chen, Y.Tang, K.Wang, C.Liu and C.Luo . *Electrochem Commun* 2011,**13**,133–7.
82 P.Yao, P.Chen, L.Jiang, H.Zhao, H.Zhu, D.Zhou, D.Hu , Han B.H., and M.Liu. *Adv Mater.* 2010,**22,**5008–12.
83 W.Gao, L.B.Alemany, L.Ci and P.M.Ajayan . *Nature Chem.* 2009,**1**,403–8.
84 J.Geng, L.Liu, S.B.Yang, S.C.Youn, D.W.Kim, D.W.Lee , J.K.Choi and H.T.Jung. *J Phys Chem C* 2010,**14**,14433–40.
85 H.He,T.Riedl,A.Lerf and J.Klinowski. *J.Phys.Chem* 1996,**100(51),**19954–8.
86 H.He,J.Klinowski,M.Forster and A.Lerf *Chem.Phys.Lett* 1998,**287(1,2)**,53–6.
87 A Lerf, H.He, T.Riedl, M.Forster and J. Klinowski. *Solid State Ionics* ,1997,**101–103(2)**,857–62.
88 A.Lerf, H.He, M.Forster and J.Klinowski. *J Phys Chem B,* 1998,**102(23)**,4477–82.
89 T.Szabo, O.Berkesi and I.Dekany. *Carbon* 2005,**43(15),**3186–9.
90 C.H.Lucas, A.J.L.Peinado, J.D.L.Gonzalez, M.L.R.Cervantes, and R.M.M.Aranda. *Carbon* 1995,**33(11),**1585–92.
91 H.C.Brown and S.Krishnamurthy. *Tetrahedron* 1979,**35**,567−607.
92 March's Advanced Organic Chemistry; Reactions, Mechanisms, and Structure, 6th ed.; John Wiley & Sons, Inc.: New Jersey, 2007
93 C.G.Lyons, S.M.Lintock and N.H.Lumb.Pergamon Press Ltd. 1965.
94 D.C.Marcano, D.V.Kosynkin, J.M.Berlin, A.Sinitskii, Z.Sun, A.Slesarev, L.B.Alemany, W.Lu and J.M.Tour. *ACS Nano* 2010,**4**,4806–14.
95 A.C.Ferrari and J.Robertson. *Physical Review B* .2000,**61(20)**,14095-140107.
96 Z.Bo, X.Shuai, S.Mao, H.Yang, J.Qian, J.Chen, J Yan. and K. Cen. Scientific Reports 2014;4:4684.
97 A.Gupta, G.Chen, P.Joshi, S.Tadigadapa and P.C.Eklund. *Nano Lett* ,2006, **6**, 2667-2673.
98 A.C.Ferrari, J.C.Meyer, V.Scardaci, C.Casiraghi, M.Lazzeri, F.Mauri, S.Piscanec, D.Jiang, K.S.Novoselov, S.Roth and A.K.Geim. *Phys Rev Lett* ,2006,97,187401.
99 P.Lespade, A.Marchand, M.Couzi and F. Cruege. *Carbon* 1984,**22**,375.
100 W.Gao, L.B.Alemany, L.Ci and P.M.Ajayan. Nat. Chem. 2009,1,403.
101 A.K.Geim and Novoselov. *Nature Mat*.2007,**6**,183-91.
102 H.M.Ju,S.H.Choi and S.H.Huh. *Journal of the Korean Physical Society*, 2010,**57(6),**1649-52.
103 H.Dong, W.Gao, F.Yan, H.Ji and H. Ju. *Anal Chem* 2010,**82**,5511-7.
104 D.Yang, A. Velamakanni, G.Bozoklu, S.J.Park, M.Stoller, R.D.Piner, S.Stankovich, I.H.Jung, D.A.Field, C.A.J.Ventrice and R.S.Ruoff. *Carbon* 2009,**47**,145-152.
105 M.Dhayal, R.Kapoor, P.G.Sistla, R.R.Pandey, S. Kar, K.K.Saini and G.Pande. *Materials Science and Engineering: C* ,2014,**37**,99-107.
106 M.Dhayal, M.R.Alexander and J.W. Bradley. *Applied surface science*. 2006,**252 (22)**,7957-7963
107 Z. Bo, X.Shuai, S.Mao, H.Yang, J. Qian, J.Chen, J.Yan and K.Cen Sci. Rep. 2014;4:4684.
108 P.K.Chu and L.Li.*Materials Chemistry and Physics* ,2006,96,253-277.
109 Y.S.Yuji, Y.Iijima, D.Asakawa and K.Hiraoka.*Surface and Interface Analysis*. 2010,**42(6-7)**,658-661.
110 Moulder JF, Stickle WF, Sobol PE, and Bomben K (J. Chastain, editor). Handbook of X-ray Photoelectron Spectroscop. Perkin-Elmer Corporation (Physical Electronics) 1992.
111 K.S.Kim and N Winograd. *Chemical Physics Letters*, 1975,**31(2),** 312-317.